ZIBELINE INTERNATIONAL™ PUBLISHING

ISSN: 2521-0890 (Print)
ISSN: 2521-0491 (Online)
CODEN: GBEEB6

Geological Behavior (GBR)

DOI: http://doi.org/10.26480/gbr.01.2024.75.81

RESEARCH ARTICLE

# UNVEILING THE GEOTHERMAL ENERGY POTENTIAL IN THE SOUTHEASTERN NIGER DELTA: INSIGHTS FROM HIGH-RESOLUTION AEROMAGNETIC DATA

**Aniekan E. Ekpo[a]*, Nsikak E. Bassey[a], Nyakno J George[b], Itoro C. Udo[a]**

*[a]Department of Geology, Akwa Ibom State University, Mkpat Enin, Akwa Ibom State, Nigeria*
*[b]Department of Physics, Akwa Ibom State University, Mkpat Enin, Akwa Ibom State, Nigeria*
**Corresponding Author Email: acdiamonmarkng@gmail.com*



**ARTICLE DETAILS**

***Article History:***

Received 23 September 2024
Revised 18 October 2024
Accepted 12 November 2024
Available online 26 December 2024

**ABSTRACT**

The geothermal energy potential in southeastern Niger Delta, Nigeria, was evaluated using high-resolution aeromagnetic data. The study examined key thermal parameters, including Curie Point Depth (CPD), Geothermal Gradient, Heat Flow, and magnetic source depths, to assess the feasibility of geothermal energy production. Results show significant spatial variations in geothermal characteristics, with some areas displaying high exploration potential. Block 9, near Akamkpa (latitude: 5.485°N, longitude: 7.035°E), has the shallowest CPD at 23.27 km, indicating strong geothermal potential due to the proximity of subsurface heat. In contrast, Block 36 near Ikot Abasi (latitude: 4.815°N, longitude: 7.049°E), with a CPD of 83.15 km, presents deeper and less accessible resources. Geothermal Gradient values range from 6.98°C/km to 24.93°C/km, with Block 9 exhibiting a higher gradient, favorable for geothermal energy extraction at shallower depths. Heat flow varies from 17.44 mW/m$^2$ to 62.33 mW/m$^2$, with Block 9 again showing the highest values, aligning with its shallow CPD and high gradient, suggesting active geothermal processes. In contrast, Block 36 demonstrates lower heat flow and geothermal potential. Magnetic source depth maps and Total Magnetic Intensity residual data also support Block 9 as a promising location for geothermal development. It is recommended that Block 9 be prioritized for further exploration, with detailed geophysical surveys like seismic and magnetotelluric (MT) studies to refine drilling targets.

**KEYWORDS**

Geothermal energy, Niger Delta, Aeromagnetic data, Curie Point Depth, Geothermal Gradient, Heat Flow

## 1. INTRODUCTION

Geothermal energy represents one of the most reliable and sustainable forms of renewable energy, providing a constant energy supply with minimal environmental impact. The growing global energy demand and increasing environmental concerns have driven interest in renewable energy sources. As one of the largest energy producers in Africa, Nigeria remains heavily reliant on fossil fuels, particularly oil and gas, for its energy needs. However, with the growing demand for clean energy and the need to diversify its energy sources, exploring alternative energy resources such as geothermal energy has gained importance. Southeastern Niger Delta, known for its hydrocarbon resources, also holds potential for geothermal energy development due to its unique geological characteristics (Eyinla et al., 2016). The transition from conventional energy sources to renewable energy has become a priority for countries worldwide as part of efforts to reduce carbon emissions and combat climate change. Fossil fuels, which account for the majority of global energy consumption, have long been associated with environmental challenges, including air pollution and greenhouse gas emissions (International Energy Agency [IEA], 2021). In response to these challenges, the exploration of renewable energy sources such as solar, wind, hydroelectric, and geothermal energy has become increasingly important.

Geothermal energy, which is derived from the Earth's internal heat, has attracted significant attention due to its reliability, low carbon footprint, and ability to provide continuous baseload power. While geothermal energy has been extensively exploited in tectonically active regions such as Iceland, Kenya, and the Philippines, recent advances in geophysical exploration techniques, such as aeromagnetic surveys, have made it possible to identify geothermal potential in areas with less obvious surface expressions, including sedimentary basins like the Niger Delta (Fridleifsson et al., 2008; Blakely, 1995).

Nigeria's energy sector is in urgent need of diversification as the country faces significant challenges in meeting its growing energy demand. The reliance on fossil fuels, particularly oil and gas, has led to environmental degradation, air pollution, and the depletion of non-renewable resources. Furthermore, the country's power generation infrastructure is inadequate, leading to frequent blackouts and energy shortages (Energy Commission of Nigeria, 2013).

Exploring the geothermal energy potential of the Southeastern Niger Delta will offer a viable solution to these challenges. Geothermal energy being a clean, sustainable, and reliable energy source that can provide continuous baseload power, reducing Nigeria's dependence on fossil fuels and contributing to its energy security (Eyinla et al., 2016). Hence, this study will examine the geothermal energy resource potential in the Southeastern Niger Delta using high-resolution aeromagnetic data to identify subsurface heat sources and geological structures that could host geothermal systems, thus contribute to the development of geothermal energy resources in the Southeastern Niger Delta, providing a new avenue for renewable energy production in Nigeria.

### 1.1 Overview of Geothermal Energy

| Quick Response Code | Access this article online | |
|---|---|---|
| | **Website:** www.geologicalbehavior.com | **DOI:** 10.26480/gbr.01.2024.75.81 |

Cite The Article: Aniekan E. Ekpo, Nsikak E. Bassey, Nyakno J George, Itoro C. Udo (2024). Unveiling the Geothermal Energy Potential in the Southeastern Niger Delta: Insights from High-Resolution Aeromagnetic Data. *Geological Behaviour 8(1): 75-81.*

Geothermal energy originates from the heat stored within the Earth's crust, primarily generated from the decay of radioactive isotopes and the residual heat from the Earth's formation. This heat is transported to the surface via conduction and convection through the Earth's mantle and crust. Geothermal energy can be harnessed by extracting hot water or steam from geothermal reservoirs located several kilometers below the surface and using it to generate electricity or provide direct heat for industrial and residential applications (Dickson and Fanelli, 2013).

**The key components of a geothermal system are:**

- Heat Source: A region of elevated temperatures within the Earth's crust, often associated with magmatic or tectonic activity.
- Reservoir: A porous or fractured rock formation that stores geothermal fluids.
- Fluid: Water or steam that transfers heat from the subsurface to the surface.
- Cap Rock: A low-permeability layer that traps the geothermal fluids and prevents them from escaping (Lund et al., 2010).

**Geothermal resources are classified based on temperature into:**

- Low-Temperature Resources: Less than 150°C, used for direct heating.
- Medium-Temperature Resources: Between 150°C and 200°C, suitable for binary power plants.
- High-Temperature Resources: Greater than 200°C, suitable for conventional geothermal power plants (DiPippo, 2008).

While high-temperature geothermal resources are typically associated with volcanic regions, the potential for medium-to-low temperature geothermal resources exists in sedimentary basins, particularly in regions with high geothermal gradients and favorable tectonic settings, such as the Niger Delta (Ajakaiye and Millar, 1985).

### 1.2 Geothermal Energy Potential in Nigeria

Nigeria's energy sector is dominated by fossil fuels, particularly oil and gas, which account for the majority of its energy production. However, the country has faced persistent challenges in meeting its growing energy demand due to the unreliable supply of electricity, aging infrastructure, and frequent power outages (Energy Commission of Nigeria, 2013). In recent years, there has been a growing recognition of the need to diversify Nigeria's energy mix, with a focus on exploring renewable energy resources such as solar, wind, and geothermal energy (Odeyemi and Ibrahim, 2020).

Geothermal energy offers several advantages for Nigeria, particularly in the Niger Delta region, where the subsurface heat flow and tectonic activity suggest favorable conditions for geothermal resource development (Eyinla et al., 2016). The Southeastern Niger Delta, which lies within a geologically active sedimentary basin, holds potential for geothermal energy exploration due to the presence of subsurface heat anomalies and geological structures conducive to geothermal reservoir formation (Emujakporue and Ekine, 2014). The region's geothermal potential is of particular interest as it could provide a sustainable alternative to fossil fuel-based energy production, contributing to Nigeria's energy security and reducing its carbon footprint.

### 1.3 Geology of The Area of Study

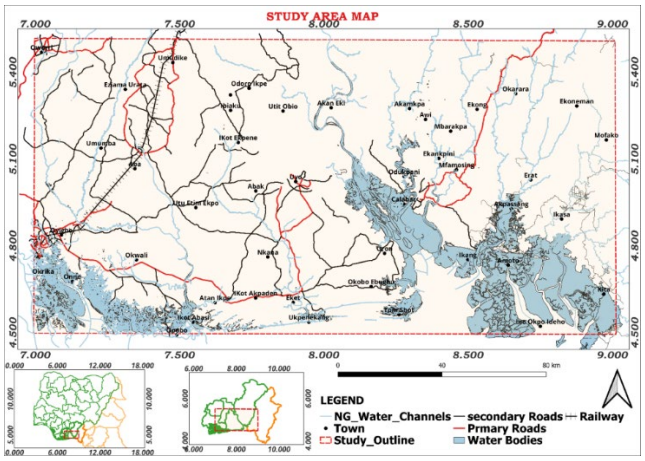


**Figure 1:** Location map of the study area.

The study location is located in Nigeria's Tertiary Niger Delta Basin's southeast onshore zone. It includes portions of the southern Nigerian states of Bayelsa, Imo, Rivers, Abia, Akwa Ibom, and Cross River. The region (Figure 1) is roughly 24,650 km$^2$ in size and is located between latitudes 4°50′N and 5°50′N and longitudes 7°00′E and 9°00′E. Figure 2 displays the region's topographic map, while Figure 3 shows its geology map.

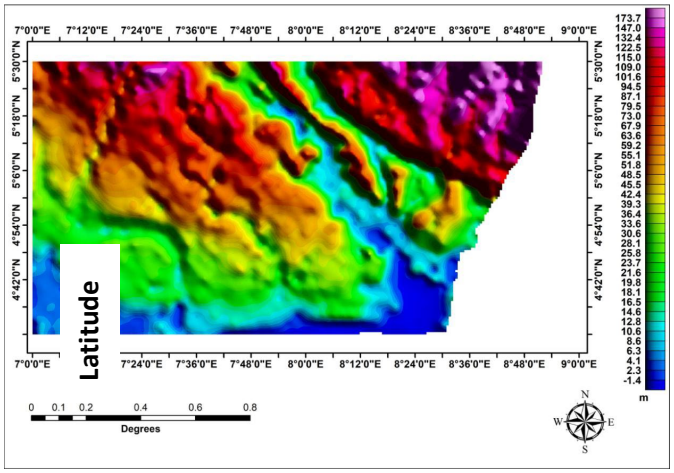


**(a)**

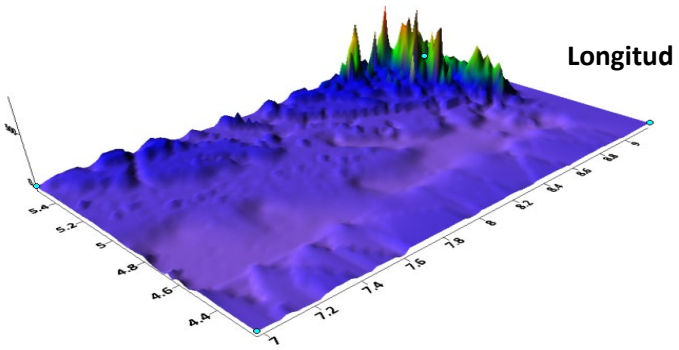


**(b)**

**Figure 2:** (a) Topographic map of the study area. (b) 3D view of topographic map of the study area (USGS).

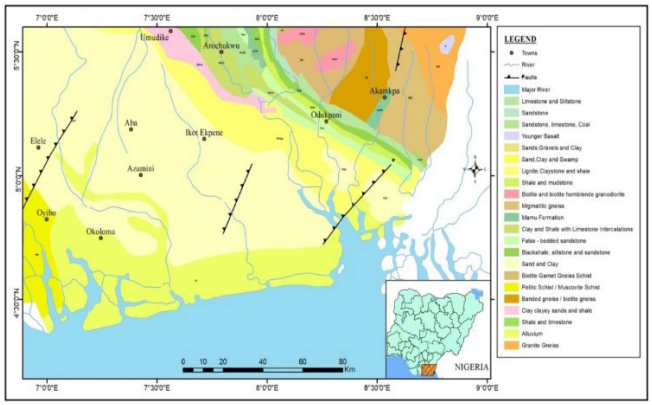


**Figure 3:** Geologic map of the study area (Ekpo et al., 2024a).

The Niger Delta Basin, located in the Gulf of Guinea along Nigeria's western coastline, is an extensional rift basin positioned on a passive continental margin. Equatorial Guinea, São Tomé and Príncipe, and Cameroon are all included in its geological framework (Tuttle et al., 2015). The basin is a prolific hydrocarbon-rich province and one of the world's largest Tertiary deltas (Doust, 1990). About 500,000 km$^3$ of sedimentary deposits make up its 300,000 km$^2$ total area, which includes a subaerial region of roughly 75,000 km$^2$ (Okiwelu et al., 2013; Tuttle et al., 2015). According to most of research study, the sediment thickness ranges from 9 to 12 km (Merki, 1972; Evamy et al., 1978; Fatoke, 2010; Okiwelu et al., 2013).

Geologically, the basin exhibits diverse formations that chronicle its evolutionary history and reflect the tectonic processes occurring at both

regional and broader scales. As an extensional basin, it shares structural similarities with other basins in the region. Some researcher describe the Niger Delta Basin as forming the southwestern edge of the extensive Benue Trough tectonic system (Lehner and De Ruiter, 1977). Its eastern boundary aligns with the Cameroon Volcanic Line and the associated transform passive margin (Fatoke, 2010). The geological setting of the Southeastern Niger Delta is marked by the presence of faults and fractures that provide pathways for fluid migration, which is essential for geothermal system formation (Reijers, 2011). Additionally, the region's tectonic activity, combined with the emplacement of igneous bodies, creates the necessary heat sources for geothermal reservoirs.

## 2. MATERIALS

The study utilized aeromagnetic data provided by the Nigerian Geological Survey Agency (NGSA). Specifically, eight (8) magnetic sheets; 321, 322, 323, 324, 329, 330, 331, and 332 were employed for this investigation. Data analysis was carried out using various software tools, including ArcGIS (version 10.1), Microsoft Excel, Oasis Montaj (version 8.4) and Surfer (version 13). These tools facilitated the efficient processing and interpretation of the aeromagnetic data.

### 2.1 Data Acquisition

Fugro Airborne Surveys, Canada, gathered the airborne magnetic data used in this investigation from 2005 to 2010. Flux-gate proton precession magnetometers combined with a Flux-Adjusting Surface Data Assimilation System were used for data collection. The surveys were conducted with a flight-line spacing of 0.1 km, tie lines spaced at 0.5 km, and a terrain clearance of 0.08 to 0.1 km, encompassing a total of 826,000 flight lines. These high-resolution potential field data offer significant improvements compared to the aero-geophysical data from the 1970s, making them highly suitable for mineral exploration, petroleum exploration, and geological mapping (Ekpo et al., 2024b).

The International Geomagnetic Reference Field (IGRF) adjustment was used to separate local magnetic anomalies from the regional magnetic field. The Earth's primary magnetic field, which is mostly produced by processes in the Earth's core, is represented by the IGRF, a worldwide mathematical model. The IGRF model was used to determine the predicted magnetic field at the survey locations, which was then subtracted from the observed data in order to make this correction. The resulting residual magnetic anomalies draw attention to noteworthy local geological features. Following processing, the data was converted into total magnetic gridded data and displayed as raster images in colour (Figure 4).

Furthermore, by centring anomalies directly above their causal bodies, the Reduction to Equator (RTE) technique was used to make the interpretation of magnetic data easier. Because of the Earth's magnetic field's inclination and declination, magnetic anomalies frequently seem skewed at lower latitudes. By computationally modifying the magnetic components' amplitude and phase, the RTE approach replicated data as though the Earth's magnetic field were vertical, as would be the case at the poles or equator. This modification made it simpler to correlate underlying structures with magnetic anomalies.

Additional processing was required. On the RTE map, residual-regional separation is carried out. For spectral analysis, the resulting residual map was split into 40 overlapping spectral blocks (Figure 4b), enabling in-depth interpretation of subsurface characteristics.

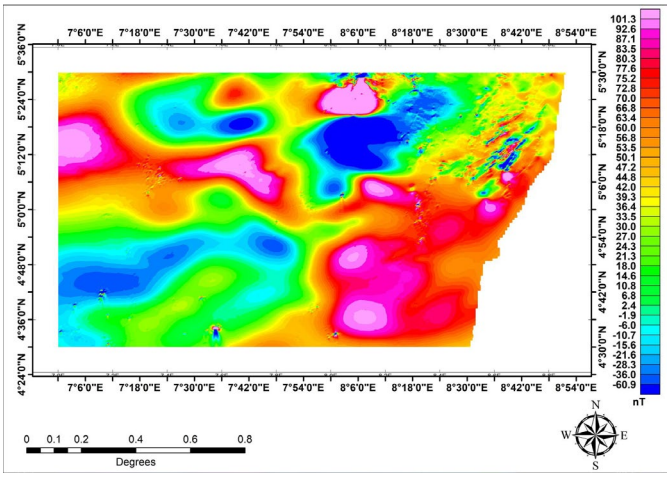


**Figure 4a:** Total magnetic intensity (TMI) map

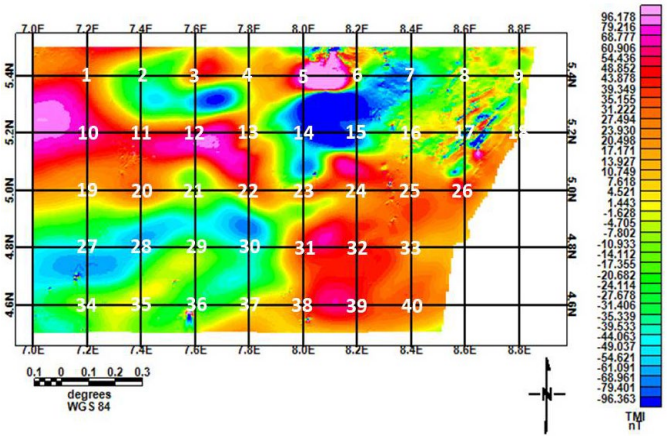


**Figure 4b:** Residual magnetic map showing 40 overlapping spectral blocks

### 2.2 Methodology

A group researcher suggested a model in which the magnetic source layer extends infinitely in all horizontal directions in order to estimate the magnetic source's Curie point depth (Zb) (Tanaka et al., 1999). This model treats the magnetisation M(x,y) as a random function of the horizontal coordinates x and y, assuming that the depth of the magnetic source correlates with its horizontal scale. According to a study, the power density spectrum of the total magnetic field anomaly (P) is mathematically represented as (Blakely, 1995):

$$P(k_x, k_y) = P(k_x, k_y) \times F(k_x, k_y) \quad (1)$$

$$F(k_x, k_y) = 4\pi^2 C_m^2 |\theta_m|^2 |\theta_f|^2 e^{-2|k|Z_t}\left[1 - e^{-|k|(Z_b - Z_t)}\right]^2 \quad (2)$$

Here, P is the magnetization's power density spectrum, $C_m$ is a proportionality constant, and θm and $\theta_f$ are the magnetization's and the geomagnetic field's respective directional factors. The depths to the top and bottom of the magnetic source layer are indicated by the variables $Z_b$ and $Z_t$. The equation is made simpler by pointing out that every term shows radial symmetry, with the exception of $|\theta_m|^2$ and $|\theta_f|^2$. Furthermore, $\theta_m$ and $\theta_f$ are constants for their radial averages.

If x is treated as a completely random and uncorrelated variable, then $k_x$, its wave number counterpart, is also constant. Consequently, the radial average of P can be simplifies to:

$$P(|k|) = Ae^{-2|k|Z_t}\left[1 - e^{-|k|(Z_b - Z_t)}\right]^2 \quad (3)$$

In this case, k is the wave number, and A is a constant. The original equation (Equation 3) can be simplified into a more straightforward expression (Equation 4) for wavelengths less than roughly twice the thickness of the magnetic source layer. The relationship between the wave number and the depth parameters is better understood thanks to this reformulation, which makes it easier to analyses the properties of the magnetic source more precisely.

$$\ln P|k|^{1/2} = \ln B - |k|Z_t \quad (4)$$

Here, B is a constant. The upper boundary of the magnetic source ($Z_t$) can be determined by fitting a straight line to the high-wave number portion of the radially averaged power spectrum [$\ln P|k|^{1/2}$]. This method allows for the estimation of $Z_t$ by analyzing the linear relationship in the spectral data, which reflects the influence of shallow magnetic sources on the observed anomalies.

$$\ln P|k|^{1/2} = Ce^{-|k|Z_0}(e^{-|k|Z_t - Z_0} - e^{-|k|Z_b - Z_0}) \quad (5)$$

Here C is a constant. With a long wavelength, equation (5) can be rewritten as;

$$\ln P|k|^{1/2} = Ce^{-|k|Z_0}(e^{-|k|(-s)} - e^{-|k|(s)}) \approx Ce^{-|k|Z_0} 2|k|s \quad (6)$$

Where 2 S is the thickness of the magnetic source. From equation (6), it can be concluded that;

$$\ln\left(\frac{P|k|^{1/2}}{|k|}\right) = \ln D - |k|Z_0 \quad (7)$$

Here, D is a constant. The centroid of the magnetic source ($Z_o$) is determined by fitting a straight line to the low-wave number portion of the radially averaged frequency power spectrum. This approach identifies the depth at which the overall magnetic effect is centered. Once the centroid depth ($Z_o$) is established, the basal depth ($Z_b$) of the magnetic source can be calculated using the following equation:

$$Z_b = 2Z_0 - Z_t \quad (8)$$

According to some studies, $Z_t$ is the depth to the top of the magnetic source, $Z_o$ is its centroid, and $Z_b$ is its basal depth, also known as the Curie point depth (Bhattacharyya and Lue, 1975; Okubo et al., 1985). Ferromagnetic minerals change into paramagnetic minerals at $Z_b$ when they reach a threshold temperature of about 580°C. The Curie point, which denotes a fundamental shift in the minerals' magnetic characteristics, is reached at this temperature.

Fourier's rule of heat conduction, which states that heat flow through a substance is proportional to the negative gradient of temperature, is the principle guiding conductive heat transfer in this application. This can be stated mathematically as:

$$q = -k\frac{dT}{dZ} \quad (9)$$

The coefficient of thermal conductivity, or k, in this case indicates how readily heat moves through a substance. $Wm^{-1}K^{-1} or\ Wm^{-1}°C^{-1}$in SI units. With a SI unit of W/m², the variable q stands for the heat flux, which is the rate of energy transfer per unit area. The temperature gradient, or dT/dZ, refers to the rate at which temperature changes in relation to depth. Heat flow is inversely proportional to the depth of a thermal isotherm, such the Curie point, as showed (Tanaka et al., 1999). According to this relationship, a deeper isotherm is produced by lower heat flow, whereas a shallower isotherm is produced by higher heat flow. Fourier's law can be simplified to the following form under the assumptions of a one-dimensional heat conduction model, in which temperature variation only happens vertically and the temperature gradient (dT/dZ) stays constant:

$$Z_b = \frac{T}{q} \quad (10)$$

Here, $Z_b$ represents the basal depth, T is the temperature at $Z_b$ (commonly the Curie temperature, approximately 580°C), and q denotes the heat flow.

In this simplified model, the assumption of a constant temperature gradient implies a linear relationship between temperature and depth. This allows for estimating the depth at which significant thermal transitions, such as the Curie point, occur by analyzing the region's thermal conductivity and heat flow.

The thermal gradient can therefore be expressed as:

$$\frac{dT}{dZ} = \frac{T_c - T_s}{Z_b} = \frac{580°C - T_s}{Z_b} \quad (11)$$

Where $T_s$ is the temperature at the surface. The Heat Flow values were calculated using equation (12)

$$q = k\left(\frac{dT}{dZ}\right) = k\left(\frac{580°C - T_s}{Z_b}\right) \quad (12)$$

Here, k is the coefficient of thermal conductivity, and q represents the heat flow. Due to the variability of rock units across the study area, the value of k may also differ depending on the specific geological formations and rock types present.

The region's geological formations have an impact on the mean value of heat conductivity within the research area. Thermal conductivity values for sedimentary basins, such as the Niger Delta, typically fall between 1.5 and 3.5 $Wm^{-1}°C^{-1}$.For example, the thermal conductivity of sedimentary rocks, including sandstones and shales, which are frequently found in the Niger Delta, is typically between 2.5 and 3.5 $Wm^{-1}°C^{-1}$ for sandstones and 1.5 to 2.5 $Wm^{-1}°C^{-1}$ for shales (Obande and Ojo, 2008; Onwuemesi and Oha, 2008). In this experiment, a thermal conductivity of 2.5 $Wm^{-1}°C^{-1}$ was employed.

## 3. RESULTS

The first set of results, derived from the spectral plot in Figure 5, is a sample from the list of other plots. The maps depicting the depth to the bottom (Figure 6), geothermal gradient (Figure 7), and heat flow (Figure 8) were analysed using the data provided in Table 1. The results for the depth to the top ($Z_t$) and depth to centroid ($Z_o$), as well as the Curie Point Depth ($Z_b$), geothermal gradient (GTG), and heat flow (HF), were all calculated using equations 8, 9, and 10 respectively.

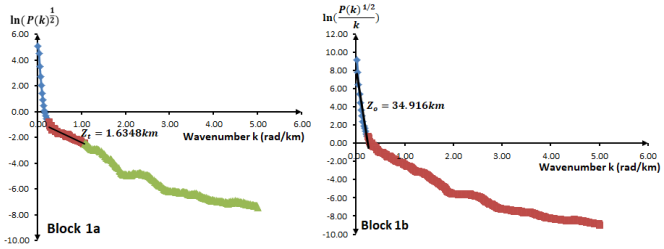


**Figure 5:** Total magnetic intensity (TMI) map

**Table 1:** Table showing Geothermal gradient, heat flow, and Average Curie Point depth computed using spectral analysis from the total magnetic intensity (TMI) map.

| Block | LONGITUDE | LATITUDE | Depth to Centriod $Z_o$ (Km) | Depth to top $Z_t$ (Km) | Curie point depth $Z_b$ (Km) | Geothermal gradient $\frac{dT}{dz}$ (°C/Km) | Heat flow Q ($mWm^{-2}$) |
|---|---|---|---|---|---|---|---|
| 1 | 7.20 | 5.40 | 34.92 | 1.63 | 68.20 | 8.50 | 21.26 |
| 2 | 7.40 | 5.40 | 28.69 | 1.94 | 55.44 | 10.46 | 26.15 |
| 3 | 7.60 | 5.40 | 32.42 | 3.46 | 61.38 | 9.45 | 23.62 |
| 4 | 7.80 | 5.40 | 30.09 | 2.32 | 57.85 | 10.03 | 25.06 |
| 5 | 8.00 | 5.40 | 30.21 | 4.20 | 56.21 | 10.32 | 25.79 |
| 6 | 8.20 | 5.40 | 28.42 | 3.48 | 53.36 | 10.87 | 27.17 |
| 7 | 8.40 | 5.40 | 29.68 | 2.31 | 57.05 | 10.17 | 25.41 |
| 8 | 8.60 | 5.40 | 17.82 | 2.51 | 33.13 | 17.51 | 43.77 |
| 9 | 8.80 | 5.40 | 12.89 | 2.51 | 23.27 | 24.93 | 62.33 |
| 10 | 7.20 | 5.20 | 37.90 | 1.12 | 74.67 | 7.77 | 19.42 |
| 11 | 7.40 | 5.20 | 35.14 | 1.41 | 68.87 | 8.42 | 21.05 |
| 12 | 7.60 | 5.20 | 22.09 | 1.66 | 42.51 | 13.64 | 34.11 |
| 13 | 7.80 | 5.20 | 29.88 | 1.73 | 58.04 | 9.99 | 24.98 |
| 14 | 8.00 | 5.20 | 26.18 | 2.37 | 50.00 | 11.60 | 29.00 |
| 15 | 8.20 | 5.20 | 27.12 | 1.64 | 52.60 | 11.03 | 27.56 |
| 16 | 8.40 | 5.20 | 34.89 | 2.50 | 67.28 | 8.62 | 21.55 |
| 17 | 8.60 | 5.20 | 19.80 | 2.35 | 37.26 | 15.57 | 38.92 |
| 18 | 8.80 | 5.20 | 18.32 | 2.56 | 34.08 | 17.02 | 42.55 |

**Table 1 (Cont.):** Table showing Geothermal gradient, heat flow, and Average Curie Point depth computed using spectral analysis from the total magnetic intensity (TMI) map.

| | | | | | | | |
|---|---|---|---|---|---|---|---|
| 19 | 7.20 | 5.00 | 39.82 | 1.48 | 78.15 | 7.42 | 18.55 |
| 20 | 7.40 | 5.00 | 25.83 | 1.51 | 50.15 | 11.56 | 28.91 |
| 21 | 7.60 | 5.00 | 31.87 | 1.50 | 62.23 | 9.32 | 23.30 |
| 22 | 7.80 | 5.00 | 30.29 | 3.12 | 57.46 | 10.09 | 25.23 |
| 23 | 8.00 | 5.00 | 32.08 | 0.92 | 63.23 | 9.17 | 22.93 |
| 24 | 8.20 | 5.00 | 32.10 | 1.02 | 63.18 | 9.18 | 22.95 |
| 25 | 8.40 | 5.00 | 39.64 | 3.64 | 75.64 | 7.67 | 19.17 |
| 26 | 8.60 | 5.00 | 28.56 | 3.07 | 54.04 | 10.73 | 26.83 |
| 27 | 7.20 | 4.80 | 40.24 | 1.47 | 79.01 | 7.34 | 18.35 |
| 28 | 7.40 | 4.80 | 34.56 | 1.16 | 67.97 | 8.53 | 21.33 |
| 29 | 7.60 | 4.80 | 31.93 | 1.26 | 62.60 | 9.26 | 23.16 |
| 30 | 7.80 | 4.80 | 37.59 | 2.05 | 73.14 | 7.93 | 19.82 |
| 31 | 8.00 | 4.80 | 31.59 | 2.46 | 60.73 | 9.55 | 23.88 |
| 32 | 8.20 | 4.80 | 39.22 | 1.89 | 76.55 | 7.58 | 18.94 |
| 33 | 8.40 | 4.80 | 36.83 | 1.75 | 71.92 | 8.06 | 20.16 |
| 34 | 7.20 | 4.60 | 26.63 | 1.14 | 52.11 | 11.13 | 27.82 |
| 35 | 7.40 | 4.60 | 40.08 | 2.29 | 77.86 | 7.45 | 18.62 |
| 36 | 7.60 | 4.60 | 42.68 | 2.22 | 83.15 | 6.98 | 17.44 |
| 37 | 7.80 | 4.60 | 35.57 | 1.57 | 69.57 | 8.34 | 20.84 |
| 38 | 8.00 | 4.60 | 34.04 | 1.41 | 66.67 | 8.70 | 21.75 |
| 39 | 8.20 | 4.60 | 33.66 | 1.30 | 66.02 | 8.78 | 21.96 |
| 40 | 8.40 | 4.60 | 27.01 | 2.36 | 51.67 | 11.23 | 28.06 |
| | **AVERAGE** | | | | **60.36** | **10.30** | **25.74** |

The Curie Point Depth (CPD) Map (figure 6), which depicts the depth at which the magnetic anomaly loses its magnetism at Curie temperature ($Tc$), has an average depth of 60.36 km. The lowest and highest values are 23.27 km (Block 9) and 83.15 km (Block 36), respectively.

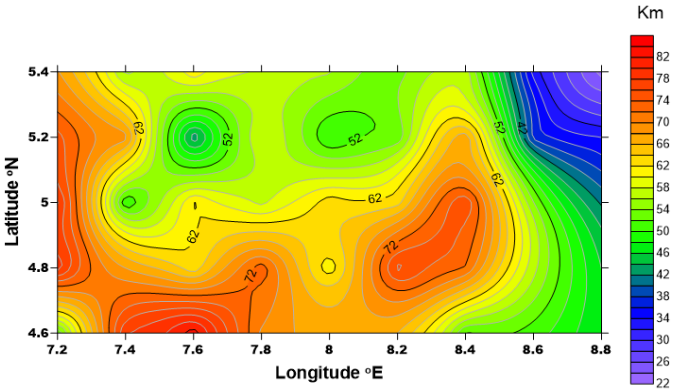


**Figure 6:** Curie point depth map

The Geothermal Gradient Map (Figure 7) shows the rate of depth dependent temperature growth ranging between 6.98 °C$km^{-1}$ to 24.93 °C$km^{-1}$with an average value of 10.30 °C$km^{-1}$.

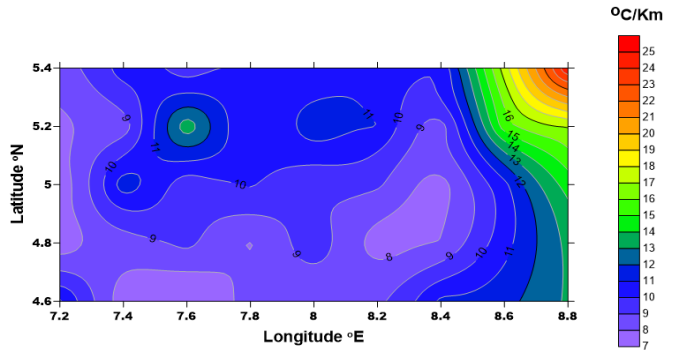


**Figure 7:** Geothermal gradient map

The Heat Flow values ranges between 17.44 $mWm^{-2}$ to 62.33 $mWm^{-2}$ [1]with an average value of 25.74 $mWm^{-2}$.

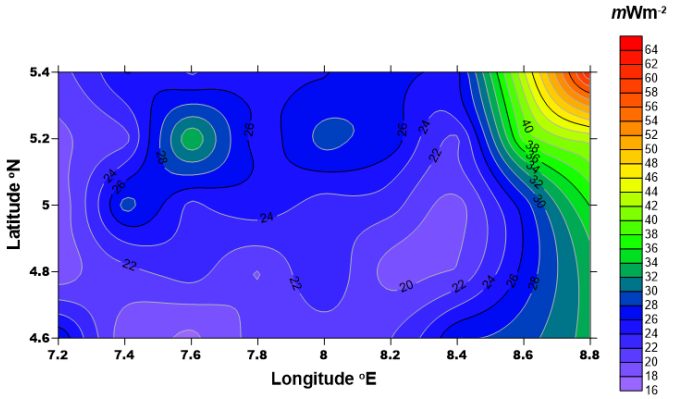


**Figure 8:** Heat flow map

The depth to centroid map (figure 9) indicates depth range from 12 km to 42 km

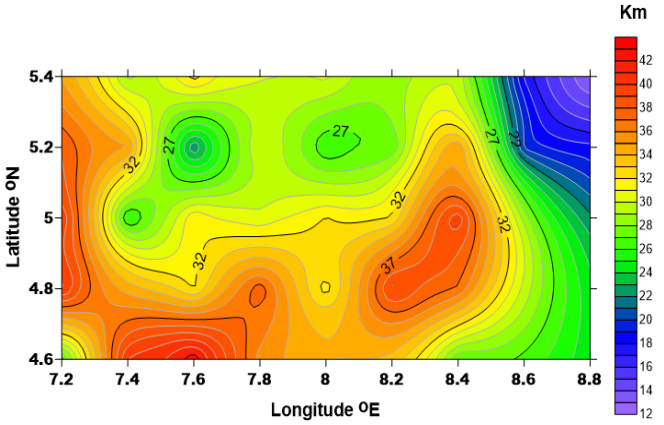


**Figure 9:** Depth to centroid of magnetic source map

Depth to the top of the magnetic map (figure 10) source in the area showed a variation between 0.8 km to 4.2 km.

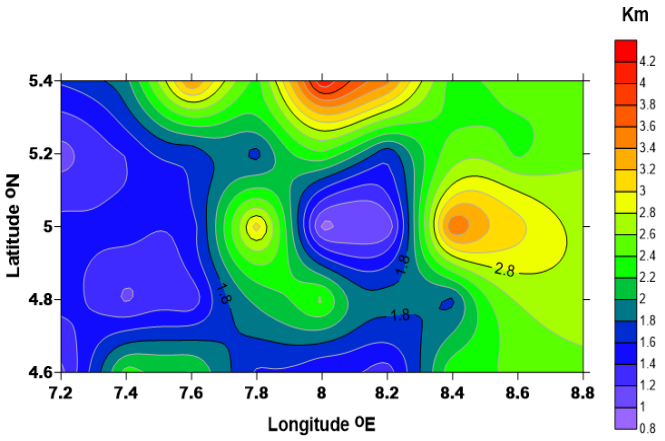


**Figure 10:** Depth to top of magnetic source map

## 4. Discussion

The assessment of the geothermal energy resource potential in parts of southeastern Nigeria using high-resolution aeromagnetic data provides a crucial insight into the subsurface thermal structure and the viability of harnessing geothermal energy. The study focuses on utilizing various maps derived from the aeromagnetic data, including the Curie Point Depth (CPD) map, Geothermal Gradient map, Heat Flow map, Depth to Centroid, Depth to Top of Magnetic Sources map. These maps, combined with the topographic and geologic context of the region, offer a comprehensive analysis of the geothermal energy prospects in the study area, which spans across different blocks within the southeastern part of the Niger Delta.

The Curie Point Depth (CPD) is fundamental in determining the thermal structure of the Earth's crust. It represents the depth at which magnetic minerals lose their magnetism due to exceeding the Curie temperature, typically around 580°C. The CPD map for southeastern Nigeria reveals a significant range in depth values, from as shallow as 23.27 km in Block 9 to as deep as 83.15 km in Block 36, with an average depth of 60.36 km. These variations suggest that certain areas have a much shallower proximity to heat sources, which are essential for geothermal exploration. Block 9, located near Akamkpa (with coordinates approximately 5.485° N, 8.795° E), emerges as a particularly promising area due to its relatively shallow CPD, indicating that the geothermal heat is more accessible in this region. In contrast, Block 36, located further to the south, has a much deeper CPD, suggesting that heat is located at significantly greater depths, making it less favorable for immediate geothermal energy extraction.

The Geothermal Gradient map further refines our understanding of how temperature increases with depth in the Earth's crust within the study area. The map revealed a wide range of geothermal gradients, from 6.98°C/km to 24.93°C/km, with an average of 10.30°C/km. Higher gradients was observed in Block 9, indicating that temperatures rise more sharply with depth, thus requiring less drilling to reach the necessary temperatures for geothermal power generation. Conversely, areas with lower geothermal gradients, such as parts of Blocks 32 to 36, would require deeper drilling to access similar temperatures. The relationship between the geothermal gradient and the CPD map emphasizes that areas with shallower Curie depths and higher geothermal gradients are more promising for geothermal development. In this context, areas around Akamkpa and its surrounding blocks offer significant potential, while regions further south may be more challenging and costlier to exploit.

The Heat Flow which is a crucial indicator of the actual geothermal potential of the region, as it measures the amount of heat escaping from the Earth's interior to the surface. Heat flow values in southeastern Nigeria range from 17.44 mW/m$^2$ to 62.33 mW/m$^2$, with an average of 25.74 mW/m$^2$. The highest heat flow values are found in Block 9, closely correlating with its shallow CPD and high geothermal gradient. These higher values suggest that the areas around Akamkpa and other northern blocks is particularly promising for geothermal energy exploitation. In contrast, southern blocks like Block 36 exhibit significantly lower heat flow values, correlating with their deeper CPD and lower geothermal gradient, suggesting that geothermal potential is less accessible in those areas. High heat flow regions are typically associated with thinner crust or tectonically active zones, where the Earth's internal heat can more readily escape to the surface, creating favorable conditions for geothermal energy production.

The Depth to Centroid of Magnetic Sources and Depth to the Top of Magnetic Sources maps provide additional structural insights that are critical for understanding the geothermal characteristics of the region. These maps help in identifying the depth at which magnetic sources are located, giving a clearer picture of the thermal regime below the surface. Shallow depths to the centroid and top of magnetic sources are often indicative of regions with higher geothermal potential, as they suggest that the heat-producing layers are closer to the surface. In southeastern Nigeria, these depths vary across the study area, with shallower depths corresponding to regions of higher heat flow and geothermal gradient. The maps align with previous findings, reinforcing that Blocks 9 and surrounding areas, which have shallower magnetic source depths, are more favorable for geothermal energy development.

Based on the temperature classifications of geothermal resources, the geothermal potential of the Niger Delta region as inferred from the aeromagnetic data can be classified according to the following temperature ranges (DiPippo, 2008):

### 4.1 Low-Temperature Resources (<150°C)

The lower end of the geothermal gradient observed in the Niger Delta (ranging from 6.98°C/km to 24.93°C/km) suggests that areas with lower geothermal gradients, such as Block 36 near Ikot Abasi, are more likely to fall into the low-temperature resource category. These areas would be suitable for direct heating applications rather than electricity generation, as their deeper Curie Point Depths (up to 83.15 km) and lower heat flow values (as low as 17.44 mW/m$^2$) indicate cooler subsurface conditions.

### 4.2 Medium-Temperature Resources (150°C – 200°C)

Blocks with intermediate geothermal gradients, around the average of 10.30°C/km, may fall into the medium-temperature resource classification. This could include areas like Block 9 near Akamkpa, where heat flow values reach 62.33 mW/m$^2$ and geothermal gradients are higher, making these regions potentially suitable for binary power plants that operate on medium-temperature resources.

### 4.3 High-Temperature Resources (>200°C)

While the analysis shows significant geothermal potential in blocks like Block 9 with shallow Curie Point Depths (23.27 km), the region does not explicitly indicate temperatures exceeding 200°C based solely on the average geothermal gradients provided. High-temperature resources, suitable for conventional geothermal power plants, would typically require even higher geothermal gradients or specific tectonic conditions, which are not clearly reflected in this data set. However, further detailed geothermal exploration could help confirm the presence of higher-temperature zones at specific depths.

## 5. Conclusion

In conclusion, the analysis of high-resolution aeromagnetic data over southeastern Nigeria reveals substantial variability in the geothermal energy potential across the region. Blocks with shallow Curie Point Depths, high geothermal gradients, and elevated heat flow values, such as Block 9 near Akamkpa, are identified as the most promising locations for geothermal exploration. These areas are characterized by favorable thermal structures, accessible heat sources, and relatively simple topography, making them attractive targets for further investigation and potential energy production. Conversely, southern blocks with deeper CPD, lower geothermal gradients, and reduced heat flow, such as Block 36, are less favorable due to the greater depths required to access the heat and the more challenging geological and topographical conditions. This detailed mapping and analysis provide a foundational framework for guiding future geothermal exploration and energy development in southeastern Nigeria.

## Recommendation

Based on the comprehensive analysis of the geothermal energy resource potential in the Niger Delta region of southeastern Nigeria using high-resolution aeromagnetic data, the following specific recommendations can be made to guide future geothermal exploration and development:

### Focus on High Potential Areas for Geothermal Exploration

The northern part of the Niger Delta, particularly Block 9, should be prioritized for geothermal energy exploration. This block has consistently demonstrated the highest geothermal potential, with a shallow Curie Point Depth (23.27 km), high geothermal gradient (up to 24.93°C/km), and elevated heat flow (62.33 mW/m$^2$). These characteristics suggest that heat

sources are relatively close to the surface, making geothermal energy extraction both technically feasible and cost-effective. Exploratory drilling should begin in this region to assess the true viability of the geothermal resource.

### Conduct Detailed Geophysical and Geological Surveys

While the high-resolution aeromagnetic data provide valuable insights into the subsurface thermal structure, further detailed geophysical surveys such as seismic and magnetotelluric (MT) surveys should be conducted in promising areas, especially Block 9. These methods will help to confirm the depth and extent of geothermal reservoirs and refine the location of exploratory drilling. Additionally, geological surveys should focus on identifying faults and fractures in the subsurface, as these features enhance permeability and fluid flow, which are critical for geothermal energy systems.

## References


Ajakaiye, D.E., Hall, D.H., and Millar, T., 1985. Interpretation of Aeromagnetic Data across the Central Crystalline Shield Area of Nigeria. Geophysical Journal of the Royal Astronomical Society, 83, Pp. 503-517. http://dx.doi.org/10.1111/j.1365-246X.1985.tb06500.x

Bhattacharyya, B.K., and Leu, L.K., 1975. Spectral analysis of gravity and magnetic anomalies due to rectangular prismatic bodies. Geophysics, 40 (6), Pp. 993–1013. https://doi.org/10.1190/1.1440593

Blakely, R.J., 1995. Potential Theory in Gravity and Magnetic Applications. Cambridge University Press.

Dickson, M.H., and Fanelli, M., 2013. Geothermal Energy: Utilization and Technology. Routledge, London. https://doi.org/10.4324/9781315065786

DiPippo, R., 2008. Geothermal power plants: principles, applications, case studies and environmental impact. 2nd ed. Amsterdam: Butterworth-Heinemann. https://lib.ugent.be/catalog/ebk01:1000000000414733. https://doi.org/10.1016/C2014-0-02885-7

Doust, H., 1990. Petroleum geology of the Niger Delta. Geological Society, London, Special Publications, 50 (1), Pp. 365–365. https://doi.org/10.1144/GSL.SP.1990.050.01.31

Doust, H., and Omatsola, E., 1990. Niger Delta. In J. D. Edwards & P. A. Santogrossi (Eds.), Divergent/Passive Margin Basins, 45, Pp. 201-238. American Association of Petroleum Geologists.

Ekpo, A.E., Bassey, N.E., George, N.J., 2024. Aero-gravity data analysis for delineating possible channels of mineralizations migration through lineament. A case study of Southeastern Niger Delta, Nigeria. AKSU Annels of Sustainable Development, 2 (1), Pp. 139-168. https://doi.org/10.60787/AASD-v2i1-35.

Ekpo, A.E., Bassey, N.E., George, N.J., and Udo, I.G., 2024. Depth to basement estimation from aerogravity data over the Southeastern part of Niger Delta region of Nigeria. Researchers Journal of Science and Technology, 4 (5), Pp. 44–66. Retrieved from https://rejost.com.ng/index.php/home/article/view/135

Emujakporue, G.O., and Ekine, A.S., 2014. Determination of Geothermal Gradient in the Eastern Niger Delta Sedimentary Basin from Bottom Hole Temperatures. Journal of Earth Sciences and Geotechnical Engineering, 4 (3), Pp. 109-114. ISSN: 1792-9040 (print), 1792-9660 (online) Scienpress Ltd, 2014

Energy Commission of Nigeria. 2013. National Energy Master Plan. Abuja: Energy Commission of Nigeria.

Evamy, B.D., Haremboure, J., Kamerling, P., Knaap, W.A., Molloy, F.A., and Rowlands, P.H., 1978. Hydrocarbon habitat of the Tertiary Niger Delta. AAPG Bulletin, 62 (1), Pp. 1–39. https://doi.org/10.1306/c1ea47b9-16c9-11d7-8645000102c1865d

Eyinla, D., Oladunjoye, M., Ogunribido, T., Odundun, O., 2016. An Overview of Geothermal Energy Resources in Nigeria. Environtropica. 12, Pp. 61-71. ISSN 1597-815X

Fairhead, J.D., 1988. Mesozoic plate tectonic reconstructions of the central South Atlantic Ocean: The role of the West and Central African rift system. Tectonophysics, 155 (1-4), Pp. 181-191.

Fatoke, A.A., 2010. Stratigraphic and structural analysis of the Niger Delta using seismic and well log data. Geological Society of America Special Papers, 477, Pp. 217–232. https://doi.org/10.1130/2010.2477

Fridleifsson, I.B., Bertani, R., Huenges, E., Lund, J., Ragnarsson, A., and Rybach, L., 2008. The possible role and contribution of geothermal energy to the mitigation of climate change. In IPCC Scoping Meeting on Renewable Energy Sources (pp. 59-80).

International Energy Agency (IEA). 2021. World Energy Outlook 2021. Paris: International Energy Agency.

Lehner, P., and De Ruiter, P.A.C., 1977. Structural history of Atlantic margin of Africa. AAPG Bulletin, 61 (7), Pp. 961–981. https://doi.org/10.1306/c1ea1d93-16c9-11d7-8645000102c1865d

Lund, J.W., Freeston, D.H., and Boyd, T.L., 2010. Direct utilization of geothermal energy 2010 worldwide review. Geothermics, 39 (3), Pp. 189-214.

Merki, P.J., 1972. Structural geology of the Cenozoic Niger Delta. In T. F. J. Dessauvagie & A. J. Whiteman (Eds.), African Geology (pp. 635–646). University of Ibadan Press.

Obande, G.E., and Ojo, O.J., 2008. Subsurface temperature distribution and heat flow in the Nigerian Niger Delta. Journal of African Earth Sciences, 52 (1), Pp. 89–95. https://doi.org/10.1016/j.jafrearsci.2008.06.006

Odeyemi, O., and Ibrahim, A., 2020. Renewable energy potential in Nigeria: The role of policy, financing, and government intervention. Energy Policy Journal, 45 (4), Pp. 39-55.

Okiwelu, F.N., Nwosu, E.O., and Nwankwo, C.C., 2013. Geophysical mapping of hydrocarbon prospects in the Niger Delta. Nigerian Journal of Physics, 25, Pp. 45–57.

Okubo, Y., Graf, R.J., Hansen, R.O., Ogawa, K., and Tsu, H., 1985. Curie point depths of the island of Kyushu and surrounding areas, Japan. Geophysics, 50 (3), Pp. 481–494. https://doi.org/10.1190/1.1441926

Onwuemesi, A.G., and Oha, I.A., 2008. Heat flow studies and geothermal energy potential in Nigeria: A case study of the Niger Delta. Journal of Energy Exploration and Exploitation, 26 (4), Pp. 211–227. https://doi.org/0144598087850228 90

Reijers, T.J.A., 2011. Stratigraphy and sedimentology of the Niger Delta. Geological Society of London Special Publications, 49 (1), Pp. 105-111.

Tanaka, A., Okubo, Y., and Matsubayashi, O., 1999. Curie point depth based on spectrum analysis of the magnetic anomaly data in east and southeast Asia. Tectonophysics, 306 (3-4), Pp. 461–470. https://doi.org/10.1016/S0040-1951(99)00072-4

Tuttle, M.L., Charpentier, R.R., and Brownfield, M.E., 2015. Tertiary Niger Delta (Akata-Agbada) petroleum system, Niger Delta Province, Nigeria, Cameroon, and Equatorial Guinea, Africa. US Geological Survey Bulletin, 2206-A, Pp. 3–20. https://doi.org/10.3133/b2206A